



Elastic and inelastic strength of singly symmetrical I-beams

Ghada M. El-Mahdy¹, Mohamed M. El-Saadawy²

Abstract

Laterally unsupported top loaded steel beams such as those found in entrances of hotel lobbies and halls that support a masonry wall do not reach their in-plane flexural capacity due to the occurrence of elastic or inelastic lateral-torsional buckling (LTB). Doubly symmetrical sections with slender webs are often selected for these beams, however, singly symmetrical sections are more efficient. In this paper the ratio of the compression flange size to the tension flange size is increasingly varied, keeping the flange material consumption constant, to obtain a higher resistance to lateral buckling of the compression flange. The AISC Specification provisions usually refer to generalized cases where the load is applied at the shear center and special cases where the load is applied at the top of the beam are always embedded in these and are not directly addressed. Special direct solutions for this problem are becoming more popular based on accurate inelastic ultimate load analysis. This paper develops a three dimensional finite element model using COSMOS/M, which is verified by available experimental results. From this model, the elastic and inelastic LTB of I-beams is determined, which is used to investigate the effect of varying the ratio of the flange sizes on the optimum performance of the beam. Slender webs are proposed and a study is made on the performance of local and global buckling and their correlation to the total ultimate load of the beam system. The main goal of this research is to present a direct solution system which provides the most economic system selection for design.

1. Introduction

Long beams that are laterally unsupported, as found in the entrance of hotel lobbies and other halls supporting a heavy wall, are top-loaded and their ultimate strength is usually governed by the lateral-torsional buckling (LTB) of the beam. These beams usually consist of built-up I-sections with deep slender webs to achieve a greater inertia in the principal plane of bending and a large compression flange to increase the resistance of the beam to LTB. The provisions of the AISC Specification (2010) are made for beams loaded at the shear center and special cases such as top loaded singly symmetric sections are embedded in these and are not directly addressed.

¹ Research Professor, Housing and Building National Research Center (HBRC), <ghadaelmahdy@yahoo.com>

² Assistant Research Professor, Housing and Building National Research Center (HBRC),
<m_massoud2002@yahoo.com>

For singly symmetric members the shear center, S , and the centroid, C , do not coincide as shown in Fig. 1. The elastic critical moment for bending of singly symmetric beams under uniform moment in the plane of symmetry can be found in Galambos (1968) or Ziemian (2010).

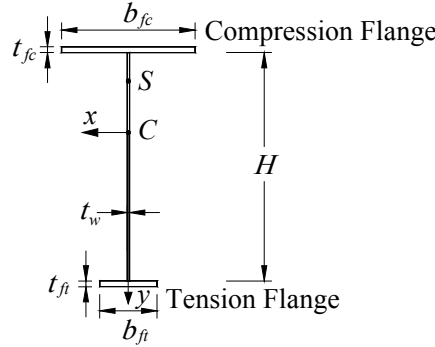


Figure 1: Singly symmetric I-section

The degree of mono-symmetry is easily given by (Kitipornchai and Trahair 1980)

$$\rho = \frac{I_{yc}}{I_{yc} + I_{yt}} = \frac{I_{yc}}{I_y} \quad (1)$$

in which $I_{yc} = t_{fc}b_{fc}^3/12$ and $I_{yt} = t_{ft}b_{ft}^3/12$ are the section minor axis second moments of area of the compression and tension flanges, respectively. The values of ρ range from 0 for a tee-beam with the flange in tension to 1 for a tee-beam with the flange in compression. For an equal flanged beam $\rho = 0.5$. When searching for the optimum flange area ratio, the degree of mono-symmetry can also be simply expressed as the ratio between the area of the compression flange A_{fc} to the total area of the flanges A_{ftot} , which is the parameter used in this study.

The AISC 360-10 Specification (2010) gives the nominal flexural strength, M_n , for doubly and singly symmetric I-shaped members with compact, noncompact, or slender webs bent about their major axis as the lowest value obtained according to the limit states of compression flange yielding, lateral-torsional buckling (LTB), compression flange local buckling, and tension flange yielding. This Specification predicts design loads that are by far unconservative for top loaded, laterally unsupported, singly symmetric I-beams. To design these sections economically direct solutions with empirical equations need to be found to ensure a safe design. In this paper elastic as well as inelastic finite element analyses are made using an eigenvalue analysis and a nonlinear analysis, respectively. The results of the nonlinear analysis are compared with the design loads specified by the AISC Specification (2010).

Several researches have been done to study the effect of applying the load above or below the shear center for singly symmetric sections (Wang and Kitipornchai 1986, Helwig et al. 1997, Mohebkhah 2011). Wang and Kitipornchai (1986) considered singly symmetric I-girders subjected to transverse loading applied at the shear center as well as at the top and bottom flanges. Energy-based solutions that considered the load height were presented for a few common load cases in single curvature bending which showed a very good accuracy for sections with $0.1 < \rho < 0.9$. Helwig et al. (1997) recommended from the results of a computational study

using the finite element method and varying the height of load application with respect to the mid-height of the section that a good estimate for the modified moment gradient factor C_b^* for the range $0.1 \leq \rho \leq 0.9$ was

$$C_b^* = C_b \left(1.4^{2y/h_o} \right) R_m \leq 3.0 \quad (2)$$

where the moment gradient factor C_b is defined in the AISC Specification (2010) as

$$C_b = \frac{12.5M_{\max}}{2.5M_{\max} + 3M_A + 4M_B + 3M_C} \quad (3)$$

where M_{\max} is the absolute value of the maximum moment in the unbraced segment and M_A , M_B , and M_C are the absolute values of the moments at the quarter, center, and three-quarter points of the unbraced segment, respectively. In Eq. 2, y is taken as the location of the applied load relative to the mid-height of the cross section, negative for loading above the mid-height and positive for loading below the mid-height, and R_m is taken as 1.0 for unbraced lengths subjected to single-curvature bending and as $(0.5 + 2\rho_{\text{op}}^2)$ for unbraced lengths subjected to double curvature bending where ρ_{op} is the value of ρ for the top flange. However, this correction to the moment gradient factor is not included in the AISC Specification (2010). Mohebkah (2011) based on a finite element analysis recommended a straight-line transition equation for the flexural resistance of beams in the inelastic range under moment gradient instead of that corresponding to that recommended by the AISC Specification (2010).

The ultimate moment for imperfect jack-beams with singly symmetric sections has been illustrated and analyzed by El-Saadawy (2015) for computing the considered lateral displacement with the corresponding ultimate vertical load.

This paper develops a three dimensional finite element model using COSMOS/M for the elastic and inelastic LTB of I-beams, which is used to investigate the effect of varying the ratio of the flange sizes on the optimum performance of the beam. The accuracy of the finite element model is verified by comparing the results to available experimental results. Slender webs are proposed and a study is made on the performance of local and global buckling and their correlation to the total ultimate load of the beam system. The flange material consumption is kept constant and only the shares to the tension and compression flanges are varied to achieve the most economical system for design. The main goal of this research is to make recommendations for the effect of mono-symmetry on the ultimate strength of singly symmetric top loaded long beams by presenting a direct solution system which provides the most economic selection for design.

2. Beams Studied

To determine the optimum ratio of flange size or the optimum degree of mono-symmetry, A_{fc}/A_{ftot} , a parametric study was conducted on singly symmetric beams with variable flange widths and constant flange thickness of 1.5 cm. The flange material consumption was kept constant with a total flange width of 50 cm and only the shares to the tension and compression flange widths were varied to obtain the most economical system for design. Table 1 shows the scheme of flange proportions taken in this study. Slender webs were used and the height of the

web was taken as 60 cm, 90 cm, and 120 cm. In all cases the same flange total area was distributed with different ratios to achieve the highest performance.

Table 1: Flange dimensions for parametric study with variable flange widths

Flange Designation	Top Flange Dimensions (cm)	Bottom Flange Dimensions (cm)	A_{fc}/A_{flot}	ρ
a	5 x 1.5	45 x 1.5	0.10	0.001
b	10 x 1.5	40 x 1.5	0.20	0.015
c	15 x 1.5	35 x 1.5	0.30	0.073
d	20 x 1.5	30 x 1.5	0.40	0.229
e	25 x 1.5	25 x 1.5	0.50	0.500
f	30 x 1.5	20 x 1.5	0.60	0.771
g	35 x 1.5	15 x 1.5	0.70	0.927
h	40 x 1.5	10 x 1.5	0.80	0.985
i	45 x 1.5	5 x 1.5	0.90	0.999
j	50 x 1.5	0 x 1.5	1.00	1.000

The web thickness was taken as 0.6 cm, giving a web height to thickness ratio (H/t_w) of 100, 150, and 200 for the web depths of 60, 90, and 120 cm, respectively. Three beam lengths were included in the parametric study to cover the normal spans in buildings, namely, 6 m, 9 m, and 12 m.

In a previous study (El-Mahdy and El-Saadawy 2015) steel grades with a yield stress of 240 and 350 MPa were studied in different combinations for the flanges and webs, however in this study the grade of structural steel used was assumed to be A572 Grade 50 with a yield stress of 345 MPa and a modulus of elasticity of 200 GPa. Hence the specimens can be designated by their length, flange proportions, and web depth (*i.e.*, 6-a-60, 12-f-120, and an asterix* denotes a variable field *etc.*).

3. Nonlinear Finite Element Model

A nonlinear inelastic finite element model was developed to investigate the elastic and inelastic LTB behavior of the singly symmetric I-beams using the finite element software package COSMOS/M 2.6 (2000). The specifications, assumptions, and verification of the finite element model are as given in the following sections.

3.1 Mesh and Material Properties

A 4-node quadrilateral thick shell element SHELL4T was used to model the web, and top and bottom flanges, as well as the stiffeners as this element has the ability to consider both geometrical and material nonlinearities. The flanges and web were modeled with a variable number of elements across the flange width and web height such that the size of the element was kept between 2.5 and 6.25 cm. In order to evenly distribute the load to the flanges and webs, vertical stiffeners were modeled at the supports with a thickness of 5 cm. In addition to the unstiffened web analysis, the case of adding vertical stiffeners to stiffen the webs was analyzed using two vertical stiffeners with a thickness of 2 cm at the third span points. Two horizontal stiffeners with a length of 0.1 the span and a thickness of 2 cm were also added at the third height points at the supports to eliminate stress concentrations in the web due to the end support. Figures 2(a) and (b) show the finite element models of the unstiffened and stiffened beam 9-f-90. An initial lateral imperfection of 1/1000 of the span length was modeled in the top flange at the

mid-span section to initiate LTB. The steel was modeled using a linear elastic perfectly plastic material model with the modulus of elasticity taken as 200 GPa and the yield stress taken as 345 MPa. No residual stresses were considered in the finite element model.

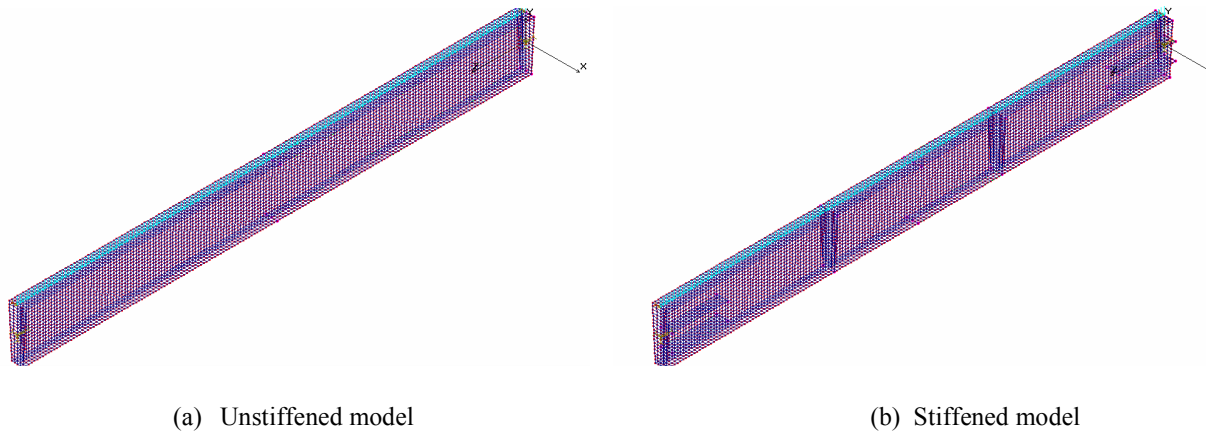


Figure 2: Finite element model of beam 9-f-90

3.2 Loads and Restraints

Simply supported end conditions were modeled at the ends of the beam at mid-height allowing for the shortening of the beam along the beam's axis at one end. Twisting of the end sections was prevented using restraints in the lateral direction of these sections. The uniformly distributed load was applied at the top flange-web junction. A full Newton-Raphson procedure was used in conjunction with a force control iterative strategy and incrementation strategy to solve the nonlinear equations. A convergence criterion based on the maximum norm of the incremental force was adopted in the incremental-iterative process; each load step consisted of the application of an increment of the external loads and subsequent iterations to restore equilibrium. The analysis ended when the time step became less than 1×10^{-4} .

In addition to the ultimate load, the finite element model was also used to obtain the bifurcation elastic buckling load using an eigenvalue analysis. The plastic moment of the section and hence the plastic load was calculated manually using a spreadsheet.

3.3 Verification of Model

The accuracy of the finite element model was verified by comparing the finite element results to experimental results available in the literature (Roberts and Narayanan 1988, Kitipornchai and Trahair 1975).

Roberts and Narayanan (1988) conducted tests on small scale model, laterally unrestrained, doubly symmetric and monosymmetric beams. The dimensions of the chosen beams are given in Table 2. The beams were simply supported and loaded by a central concentrated load acting on the top flange. The end support brackets were designed to provide simply supported conditions with respect to the lateral displacement and vertical displacement. The load was applied by weights placed on a load hanger and hence did not provide any restraint against lateral displacement. The material properties of the flange were a yield strength of 245 MPa and a modulus of elasticity of 213 GPa, whereas the material properties of the web were a yield strength of 157 MPa and a modulus of elasticity of 198 GPa. The initial geometrical imperfection

was taken as 1/1000 of the span. From the results in Table 2, it can be seen that the ultimate load obtained from the experimental tests compares well with the ultimate load obtained from the finite element model having a maximum difference of approximately $\pm 6.8\%$.

Kitipornchai and Trahair (1975) conducted tests on full scale doubly symmetric rolled steel I-beams. Tests were carried out on simply supported 10UB29 beams with central concentrated loads. The load was applied through a loading yoke which practically eliminated any restraining effects of the applied load. The actual beam dimensions of the two specimens chosen for comparison are given in Table 2. The flange yield stress was 302 MPa whereas the web yield stress was 357 MPa, and the overall modulus of elasticity was taken as 203 GPa. An initial geometrical imperfection of 1/1000 of the span was assumed. As given in Table 2, the maximum difference between the experimental ultimate load and the finite element ultimate load is approximately -4.4%. Hence it can be concluded that the finite element model gives relatively accurate results.

Table 2: Comparison of finite element results with experimental results

	Model	Span (mm)	Top Flange Dimensions (mm)	Bot. Flange Dimensions (mm)	Web Dimensions (mm)	Expt. Load (kN)	FE Load (kN)	Expt./FE Load
Roberts and Narayanan (1988)	M1	1200	25x1.53	15x1.53	60x1.0	0.735	0.732	1.004
	M2	1500	25x1.51	15x1.53	60x1.0	0.440	0.412	1.067
	M4	1000	25x1.51	15x1.52	60x1.0	1.135	1.063	1.068
	M5	1300	25x1.52	15x1.53	60x1.0	0.599	0.613	0.977
	M6	1600	25x1.51	15x1.53	60x1.0	0.395	0.380	1.040
Kitipornchai and Trahair (1975)	S2-10	3050	151.5x12.3	151.5x12.3	248.9x7.67	194.0	194.1	1.000
	S3-12	3660	151.6x12.2	151.6x12.2	248.8x7.62	140.2	146.6	0.956

4. Discussion of Results

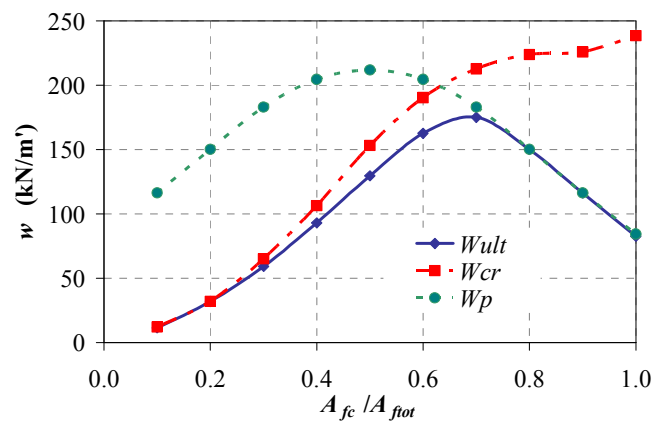


Figure 3: Critical, plastic and ultimate loads for beam 6*-60

In general, the ultimate load w_{ult} obtained through the nonlinear finite element analysis was lower than both the elastic critical load w_{cr} obtained from the bifurcation analysis, and the plastic load w_{pl} calculated for the finite element model as shown in Fig. 3. This figure shows the results for the beam with a span of 6 m and a web height of 60 cm and variable flange widths. This is

because the elastic critical load does not include the effects of inelasticity and the plastic load does not include the effect of LTB and hence the ultimate load interacts between the two. It should be noted that, ideally, the ultimate load curve approaches the plastic load curve on the right tangentially and approaches the critical elastic curve to the left asymptotically when no post buckling occurs. The ultimate load curve slightly overlaps the critical elastic curve due to the occurrence of a little post-buckling. From Fig. 3 it can also be seen that the plastic load curve peaks at a flange ratio of $A_{fc}/A_{ftot} = 0.5$, which represents a doubly symmetric section, whereas, the ultimate load peaks at a flange ratio of approximately 0.7.

4.1 Comparison of FE Results with AISC Design Loads

The nominal flexural strength M_n and hence the nominal uniformly distributed design load w_n were calculated using the AISC 360-10 Specification (2010). This included sections with compact, noncompact and slender webs. The governing lowest value obtained according to the limit states of compression flange yielding, LTB, compression flange local buckling, and tension flange yielding was taken as the design load. In general, the governing failure mode according to the AISC Specification was LTB for the beams with an A_{fc}/A_{ftot} ratio of less than 0.6 although this increased to 0.7 and 0.8 for the longer beams with a span of 9 and 12 m, respectively. For the higher A_{fc}/A_{ftot} ratios the governing failure mode was either that of compression flange local buckling or tension flange yielding reaching the plastic moment.

The design load according to the AISC Specification is compared to the ultimate load obtained from the nonlinear finite element analysis in Figs. 4-6. It can be seen from these figures that the AISC design loads are very unconservative for the unstiffened beams with a web depth of 90 and 120 cm. The nonlinear finite element analysis was repeated using vertical stiffeners at the third points along the span, as shown in Fig. 2(b), to decrease the deformation of the slender web thus increasing the stiffness of the tension flange. As shown in Figs. 4-6(b) and (c), the stiffeners increased the ultimate loads although the results were still slightly unconservative compared to the AISC design value for the beams with an A_{fc}/A_{ftot} ratio of greater than 0.4 or 0.5. Stiffening the beams with a web depth of 60 cm did not have a significant effect on the ultimate load except for the case of the 12 m span beam as shown in Figs. 4-6(a). In general, the AISC results were comparable to the finite element results of the unstiffened beams for the beams with a web depth of 60 cm.

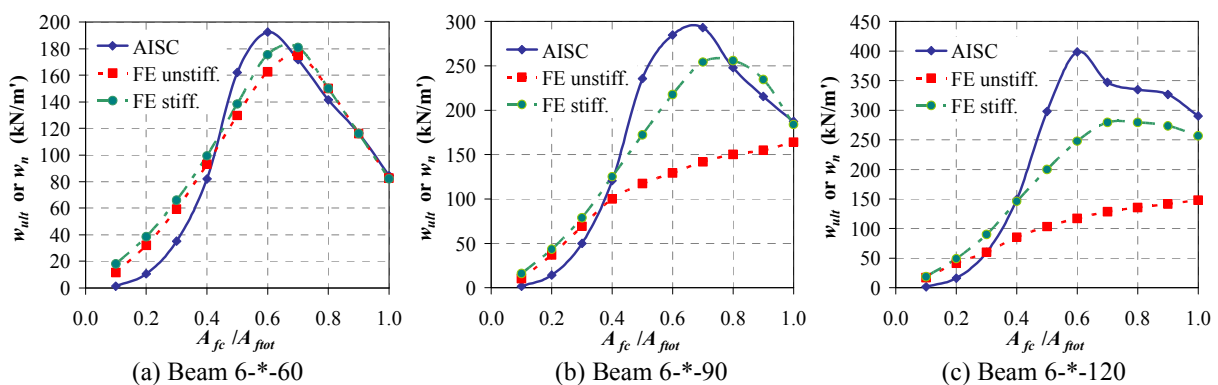


Figure 4: Comparison of AISC design results with finite element ultimate loads for beams with 6 m spans

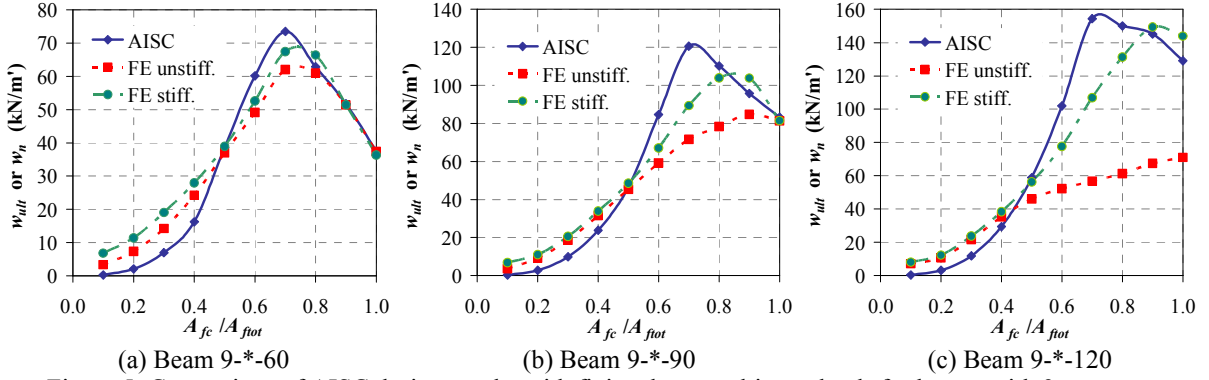


Figure 5: Comparison of AISC design results with finite element ultimate loads for beams with 9 m spans

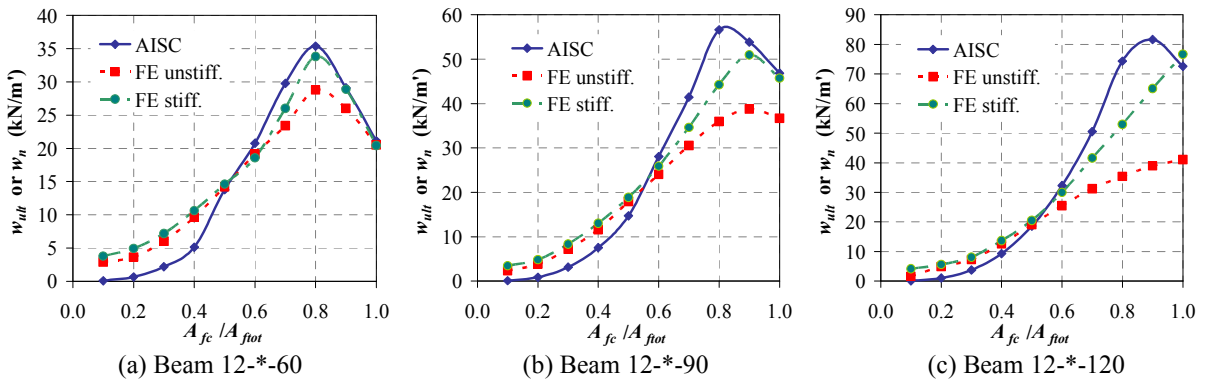


Figure 6: Comparison of AISC design results with finite element ultimate loads for beams with 12 m spans

From Figs. 4-6 it can be seen that the peak ultimate loads for the unstiffened and stiffened beams varied from an A_{fc}/A_{ftot} ratio of 0.7 to 1.0, whereas those predicted by the AISC varied from an A_{fc}/A_{ftot} ratio of 0.6 to 0.8. However, in this study the optimum ratio of the area of the compression flange to the total area of the flanges will be taken as 0.7 corresponding to flange designation ‘g’ given in Table 1.

4.2 Lateral Deflection of the Compression Flange

Studying the load-deflection curves for the lateral deflection of the compression flange and the mid-span vertical deflection gives an idea of the mode of failure of each beam. For example, Figs. 7(a)-(d) show these deflections for the unstiffened and stiffened beams with a span length of 9 m and web depth of 90 cm and an A_{fc}/A_{ftot} ratio of 0.2, 0.5, 0.8, and 1.0, respectively. The stiffened beams reached greater ultimate loads with the exception of beam 9-j-90 shown in Fig. 7(d) which reached the plastic moment load in both cases. The stiffened beams also exhibited a reduction in lateral deflection of the compression flange. From Figs. 7(a) and (b) it is obvious that LTB is the mode of failure for these beams as the lateral deflection of the compression flange by far exceeds the mid-span vertical deflection, which showed very little nonlinear behavior. Whereas, Fig. 7(c) shows that the mode of failure is LTB with tension flange yielding as the lateral deflection of the compression flange is nonlinear but is nearly equal to the mid-span vertical deflection. Finally, Fig. 7(d) shows that the mode of failure is definitely tension flange yielding as the mid-span vertical deflection exhibits nonlinear behavior and by far exceeds the lateral deflection of the compression flange.

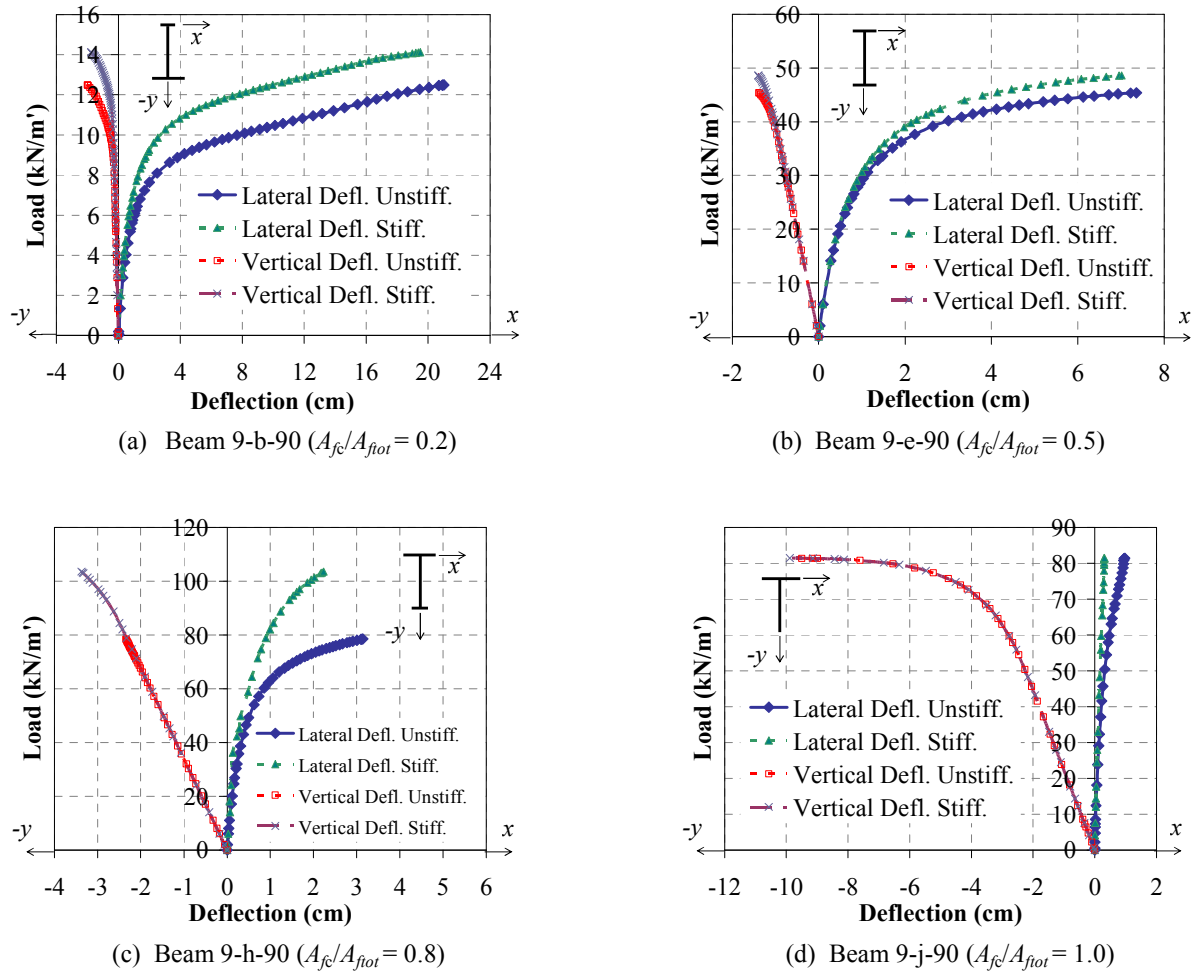


Figure 7: Load-deflection curves for lateral deflection of the compression flange and vertical deflection at mid-span

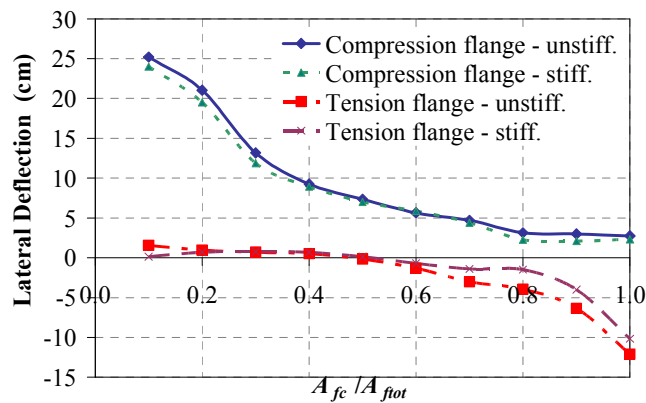


Figure 8: Lateral deflection of the compression and tension flange at the ultimate load for beam 9-*-90

A notable result of varying the size of the tension and compression flanges is the change in lateral deflection of these flanges. Figure 8 shows the variation in the lateral deflection of the compression and tension flanges with varying flange ratios for the unstiffened and stiffened beams with a span length of 9 m and a web depth of 90 cm. It can be seen that increasing the size

of the compression flange decreases the lateral deflection due to LTB with the maximum lateral deflection of the compression flange being at an A_{fc}/A_{ftot} ratio of 0.1. Increasing the width of the top compression flange at the expense of the bottom tension flange caused the lateral deflection of the upper flange to decrease at the recommended flange ratio of upper flange to total flange area of 0.7 to a value of approximately 4.5 cm at the ultimate load. Also, increasing the width of the top compression flange at the expense of the bottom tension flange caused the lateral deflection of the tension flange to increase considerably in the negative sense with respect to that of the upper compression flange, especially for the case of a tee-section with an A_{fc}/A_{ftot} ratio of 1.0 where the lateral deflection of the tension flange reached -12 cm for the unstiffened beam and -10 cm for the stiffened beam.

4.3 Longitudinal Normal Stresses

Figure 9 shows the longitudinal normal stresses at mid-span at the ultimate load for the beams with a span of 9 m, an A_{fc}/A_{ftot} ratio of 0.3 and 0.7, and web depths of 60, 90, and 120 cm. The stresses of both the unstiffened and stiffened beams are plotted together for comparison. For the beams with an A_{fc}/A_{ftot} ratio of 0.3 the unstiffened and stiffened beams show very similar results and the stresses are quite low due to the occurrence of elastic LTB at a small load. For the beams with an A_{fc}/A_{ftot} ratio of 0.7 the stiffened beams in general reach higher stresses than the unstiffened beams.

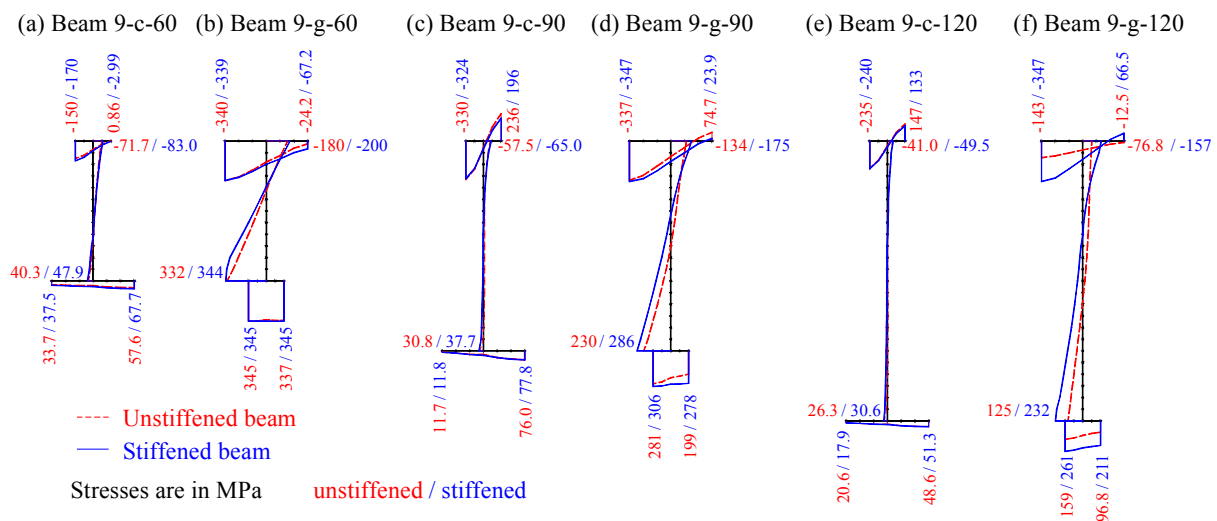
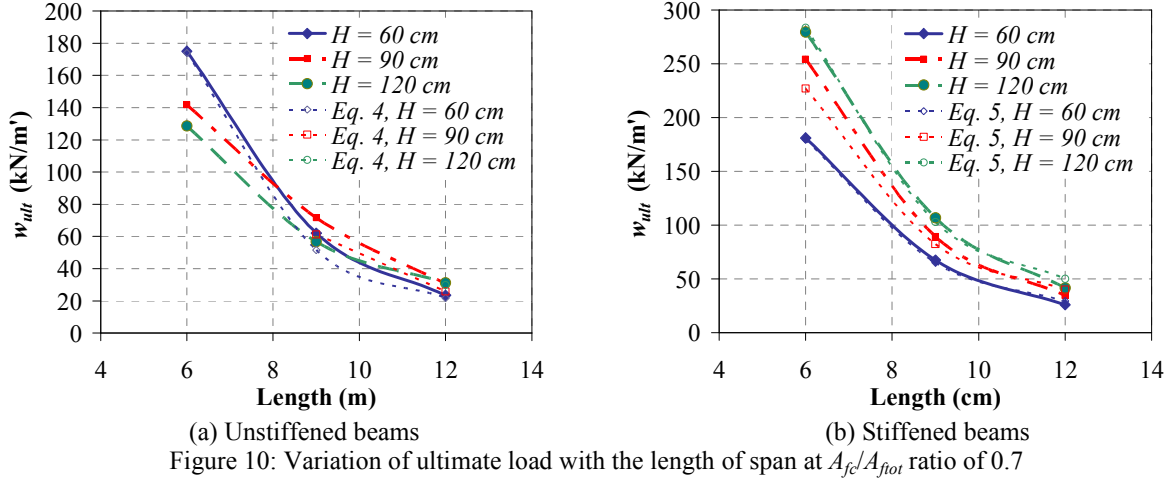


Figure 9: Longitudinal normal stresses at mid-span at the ultimate load

4.4 Approximate Design Expressions for the Ultimate Load

From the ultimate load values shown in Figs. 4-6 it is recommended that the design area of flange ratio, A_{fc}/A_{ftot} , be taken in the range of 0.7-1.0 to give the maximum ultimate load. In this study the optimum area of flange ratio is taken as 0.7 to limit the lateral deflection of the lower tension flange. Figures 10(a)-(b) show the ultimate load plotted against the span of the beam at an area of flange ratio of 0.7 for the stiffened and unstiffened beams, respectively. It should be noted that for the unstiffened beams shown in Fig. 10(a) the ultimate load for the web depth, H , of 60 cm exceeds that for a web depth of 90 cm and 120 cm for the 6 m span due to the occurrence of distortions in the slender webs. It can also be seen that the ultimate loads for the unstiffened beams with a web depth of 120 cm falls below those for the beams with a web depth

of 90 cm for the shorter spans also due to distortions in the slender web. For this reason it is recommended that the range of the span to web depth ratio, L/H , be taken greater than 8 for the unstiffened beams. These irregularities do not occur in the stiffened beams shown in Fig. 10(b) where the ultimate loads are consistent with the web height and the span and so no limitations to the span to web depth ratio are made.



Curve fitting the relationships given in Figs. 10(a) and (b) leads to analytical expressions which give relatively accurate results for the ultimate load (kN/m') as a function of the length of the beam L in meters and the depth of the web plate H in meters as follows:

$$\text{for the unstiffened beams} \quad w_{ult} = \frac{23500}{L^3}(1 + H) \quad \text{for} \left(\frac{L}{H} \right) \geq 8 \quad (4)$$

$$\text{for the stiffened beams} \quad w_{ult} = \frac{10800}{L^{2.5}}(1 + H^{1.5}) \quad (5)$$

The values obtained from the approximate formulas given in Eqs. 4 and 5, are compared to the finite element results in Figs. 10(a) and (b), respectively.

5. Conclusions

The nonlinear elastic and inelastic LTB behavior of top-loaded singly symmetric built-up steel I-section beams with variable span lengths, depths, and degrees of mono-symmetry was studied by means of the finite element method. The main aim was to study the optimum performance of these beams and make direct design recommendations for practicing engineers. The mono-symmetry of the section was varied by using variable flange widths keeping the total area of the flanges constant for comparison. It was found that increasing the top compression flange did increase the inelastic ultimate load of the beam with the ideal ratio of the area of the compression flange to the total area of flanges being in the range of 0.7-1.0. Furthermore, it was found that using variable flange widths had a definite effect on the lateral deflections of the flanges. Increasing the width of the top compression flange at the expense of the bottom tension flange caused the lateral deflection of the upper flange to decrease. Also, an increase of the compression flange width at the expense of the tension flange caused the lower tension flange lateral

deflection to increase considerably in the negative sense with respect to that of the upper compression flange.

Initially, the finite element results compared poorly with the AISC design loads being severely unconservative for the more slender webs with a web depth of 90 cm and 120 cm. This led to the stiffening of the web of the beams using two vertical stiffeners at the third points of the span and two horizontal stiffeners at the supports. The stiffened beams gave ultimate loads that were, in general, still slightly unconservative compared to the AISC design loads but comparable to these loads. To facilitate the design of singly symmetric I-sections, and based on the finite element results, an approximate formula for the ultimate load for span length to web depth ratios of greater than 8 is suggested for the unstiffened beams as a function of the beam's length and web depth, which prevents distortions of the web and secures an economical solution. A second formula is suggested for the stiffened beams also as a function of the beam's length and web depth. These formulae give accurate enough results for the ultimate load and may be used for the design of top loaded singly symmetric I-beams by using the appropriate safety factor given in the AISC Specification.

References:

- American Institute of Steel Construction (AISC). (2010). "Specification for structural steel buildings, ANSI/AISC 360-10." AISC, Chicago, IL, USA.
- COSMOS/M (2000). "COSMOS/M user's guide: version 2.6." Structural Research and Analysis Corporation, USA.
- El-Mahdy, G.M., El-Saadawy, M.M. (2015). "Ultimate strength of singly symmetric I-section steel beams with variable flange ratio." *Thin-Walled Structures*, 87 149-157.
- El-Saadawy, M.M. (2015). "Strength of jack-beams with slender webs and mono-symmetric sections." *HBRC Journal*, 11 (1), in press.
- Galambos, T.V. (1968). "Structural members and frames." Prentice-Hall, Upper Saddle River, NJ, USA.
- Helwig, T.A., Frank, K.H., Yura, J.A. (1997). "Lateral-torsional buckling of singly symmetric I-beams." *Journal of Structural Engineering*, ASCE, 123 (9) 1172-1179.
- Kitipornchai, S., Trahair, N.S. (1975). "Inelastic buckling of simply supported steel I-beams." *Journal of the Structural Division*, ASCE, 101 (ST7) 1333-1347.
- Kitipornchai, S., Trahair, N.S. (1980). "Buckling properties of mono-symmetric I-beams." *Journal of the Structural Division*, ASCE, 106 (ST5) 941-958.
- Mohebkah, A. (2011). "Lateral buckling resistance of inelastic I-beams under off-shear center loading." *Thin-Walled Structures*, 49 (3) 431-436.
- Roberts, T.M., Narayanan, R. (1988). "Strength of laterally unrestrained monosymmetric beams." *Thin-Walled Structures*, 6 (4) 305-319.
- Wang, C.M., Kitipornchai, S. (1986). "Buckling capacities of mono-symmetric I-beams." *Journal of Structural Engineering*, ASCE, 112 (11) 2373-2391.
- Ziemian, R.D. (2010). "Guide to stability design criteria for metal structures." 6th ed., John-Wiley & Sons Inc., Hoboken, NJ, USA.